ICSO 2016

International Conference on Space Optics

Biarritz, France

18–21 October 2016

Edited by Bruno Cugny, Nikos Karafolas and Zoran Sodnik

Experimental demonstration of reduced tilt-to-length coupling by using imaging systems in precision interferometers

M. Tröbs

M. Chwalla

K. Danzmann

G. Fernández Barránco

et al.

esa icso proceedings cnes

International Conference on Space Optics — ICSO 2016, edited by Bruno Cugny, Nikos Karafolas, Zoran Sodnik, Proc. of SPIE Vol. 10562, 1056245 · © 2016 ESA and CNES
CCC code: 0277-786X/17/$18 · doi: 10.1117/12.2296137

EXPERIMENTAL DEMONSTRATION OF REDUCED TILT-TO-LENGTH COUPLING BY USING IMAGING SYSTEMS IN PRECISION INTERFEROMETERS

M. Tröbs[1], M. Chwalla[2], K. Danzmann[1], G. Fernández Barránco[1], E. Fitzsimons[2,3], O. Gerberding[1], G. Heinzel[1], C. J. Killow[4], M. Lieser[1], M. Perreur-Lloyd[4], D. I. Robertson[4], S. Schuster[1], T. S. Schwarze[1], H. Ward[4] and M. Zwetz[1]

[1] Max Planck Institute for Gravitational Physics (Albert Einstein Institute) and Institute for Gravitational Physics of the Leibniz Universität Hannover, Callinstr.38, 30167 Hannover, Germany, michael.troebs@aei.mpg.de. [2]Airbus DS GmbH, Claude-Dornier-Straße, 88090 Immenstaad, Germany. [3]present address: UK Astronomy Technology Centre, Royal Observatory Edinburgh, Blackford Hill, Edinburgh EH9 3HJ, UK. [4]SUPA, Institute for Gravitational Research, University of Glasgow, Glasgow G12 8QQ, Scotland, UK.

I. INTRODUCTION

Angular misalignment of one of the interfering beams in laser interferometers can couple into the interferometric length measurement and is called tilt-to-length (TTL) coupling in the following. In the noise budget of the planned space-based gravitational-wave detector evolved Laser Interferometer Space Antenna (eLISA) [1, 2] TTL coupling is the second largest noise source after shot noise [3]. Imaging systems are foreseen to reduce TTL coupling to a level acceptable for eLISA. The requirement on the imaging systems is that they should suppress TTL coupling to less than ±25 µm/rad for beam angles within ±300 µrad. The beam angles are measured on the optical bench, the main optical instrument of eLISA, where the interferometric measurements are performed. Light exchange between satellites is accomplished by telescopes that send and receive light.

Recently, a proof-of-principle experiment was reported on that demonstrated a reduction in tilt-to-length coupling by a two-lens imaging system [4]. This investigation was not fully representative because it did not include effects of higher-order modes and different beam parameters of the interfering beams.

We describe the design and the build of a test-bed to experimentally investigate tilt-to-length coupling in a way as representative as possible for eLISA and present first results of imaging system tests. A detailed description of the design and build of the test bed is given in [5].

II. EXPERIMENTAL SETUP

A. Principle of operation

A simplified schematic of the test bed is shown in Fig. 1. The test bed comprises of two parts, an optical bench (OB) (right) and a telescope simulator (TS) (left). The first is a representation of the main optical instrument on board the eLISA satellites, the latter is a tool to characterize the OB. The TS produces a tiltable beam (Rx, green) and provides a reference interferometer. Two actuated mirrors on the TS tilt the beam around the Rx clip on the OB in the same way as a beam received by a telescope on board an eLISA satellite would be tilted. On the OB the Rx beam is interfered with a part of the local transmit (Tx, red) beam in the science (or measurement) interferometer where both beams are detected by photo diodes in both output ports. The imaging systems to be tested are the devices under test (DUT) that are placed in front of the photo diodes on the OB. The TS delivers an additional, static beam (LO, blue) that is used as alignment and phase reference. That LO beam will not be present in eLISA but is an auxiliary tool for these measurements. A fraction of the Tx beam is split off before the interference with the Rx beam and is sent to the TS. Polarising beam splitters on OB and TS are used to separate Tx and Rx beams. Both interferometers (reference and measurement) are illuminated with all three beams (LO, Tx and Rx). This leads to three interference signals: A: Rx-Tx, B: LO-Tx, C: Rx-LO. Tilt-to-length coupling is evaluated by tilting the Rx beam and measuring the length change in signal A (Rx-Tx) between reference and measurement interferometer. This requires that there be no TTL coupling in the reference interferometer on the TS. This is achieved by matching the distance from the actuators to the reference detector (with mm accuracy) to the distance to the Rx clip - not the optical pathlength $\Sigma_i n_i d_i$ but $\Sigma_i d_i/n_i$ where n_i is the refractive index and d_i is the geometrical length of segment *i*. The latter quantity is relevant for the mode propagation of Gaussian laser beams and higher orders.

The tiltable Tx beam produced by the TS can either be a Gaussian or a flat-top beam. The Gaussian beam represents the beam reflected at a test mass on the local satellite. The distance from beam rotation point to imaging system is similar for inter-spacecraft measurement as for the test mass measurement in the current eLISA design. The flat-top beam represents the beam received from a far spacecraft. Hence the test bed can be used for representative investigations of TTL coupling in the inter-spacecraft measurements and in the test mass measurements.

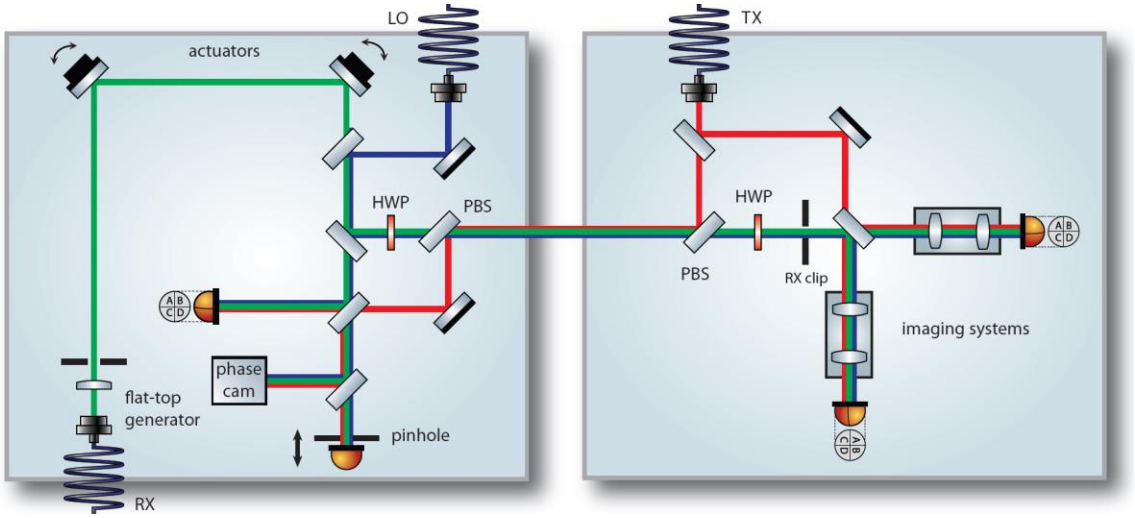

Fig. 1 Schematic of the test bed concept. The Telescope Simulator (left) and Optical Bench (right) are shown with the key components to illustrate the measurement concept. The Rx beam is shown in green, the LO beam in blue and the Tx beam in red. The Rx beam is tilted around the middle of the Rx clip with the two actuators and the pinhole photo diode is placed at the same optical distance as the Rx clip. The beams between the two baseplates have different polarizations and are separated by polarising beam splitters (PBSs). On the optical bench the imaging systems are placed in the science interferometer in front of the photo diodes in both output ports.

B. Laser preparation and interferometer phase readout

Fig. 2 shows an overview of the experimental setup. The beam of a Nd:YAG laser is split into three parts. Each part is frequency shifted by acousto-optical modulators (AOMs), driven by RF frequency generators. The Rx and Tx beams are reflected at piezo actuated mirrors. These are used for offset phase locks between the respective beams with the LO beam. The error signals for these control loops are generated at the reference interferometer on the TS. The signal between LO and Rx is kept constant by stabilizing the length of the Rx path to that of the LO path. This removes any path length errors introduced by the tilt actuators on the TS. Additionally, the length of the Tx path is adjusted to that of the LO path. In this way, the static, stable LO beam becomes the phase reference for the experiment. The LO, Rx and Tx beams are coupled into optical fibers and sent to TS and OB, respectively. The photo detectors at the interferometer output ports are read out by a LISA Pathfinder style phasemeter [6]. Its hardware is described in Sec. C of [7]. LISA Pathfinder is a technology precursor mission to an eLISA mission [8]. The phasemeter also actuates the piezo mounted mirrors within the offset phase locks.

C. Optical bench and telescope simulator design

The OB components are laid out on a Zerodur® glass-ceramic baseplate of diameter 580 mm, thickness 80 mm and mass 55 kg, obtained for an earlier design of the experiment that would have required a greater density of optical components [9, 10]. The baseplate thickness had been chosen to minimise bending, to ensure satisfactory positional stability of all mounted components throughout the build and also measurement accuracy during testing. Mounting of the baseplate is via three 20 mm diameter chrome steel ball-bearings that are glued into hemispherical cutaways in the bottom surface of the substrate. These steel ball-bearings are in contact with mating features in a metal kinematic interface plate.
The optical layout is shown in Fig. 3. The Tx beam (red) is emitted from a stable fiber injector labelled Tx FIOS. A fraction of the beam is sent to a power monitor (Tx PWR). Then the beam is split and one half is sent to the TS. The other half is interfered at BS21 with light from the TS and detected by photo detectors SciQPD1 and SciQPD2. The imaging systems under test are placed between recombination beam splitter and photo detectors. Light from the TS is reflected by the central out-of-plane mirror on the OB (TS interface). Before the interference with the Tx light, a fraction of the light is sent to two quadrant photo diodes (QPDs) labelled CQP1 and CQP2. These act as alignment aid much like a calibrated quadrant photo diode pair (CQP) [11]. These were fixed and aligned during manufacture such that any beam from the TS intersecting at the centre of both QPDs would then optimally complete the measurement interferometer. Optical components such as mirrors and beam splitters are manufactured from Corning 7980 HPFS Class 0 fused silica with tight control over the surface parallelism of the optical surfaces - 2 arc-seconds - and perpendicularity of the bottom surface - 2 arc-seconds - to facilitate the precision hydroxide-catalysis bonding [12].

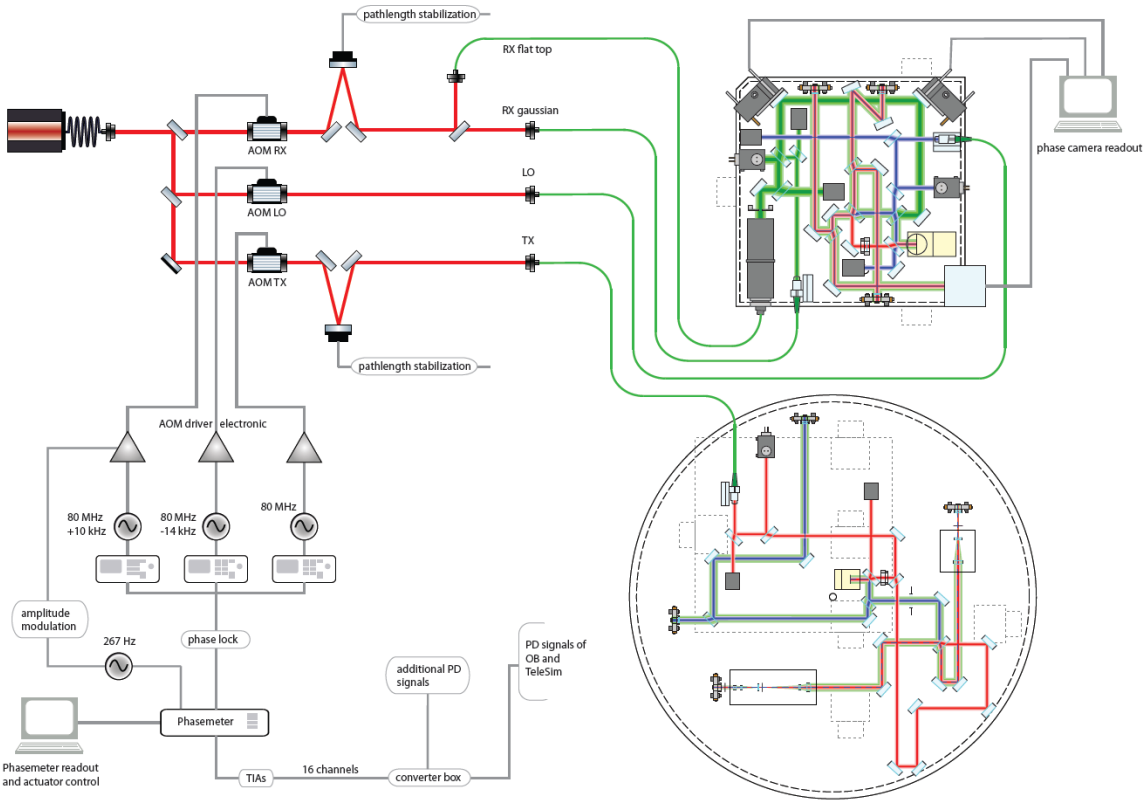

Fig. 2 Overview of the experimental setup; Schematic of the laser preparation and electronic setup for the heterodyne frequency generation and the phase readout and optical designs of optical bench and telescope simulator. A frequency stabilized laser is split into three modulation arms where the frequency is shifted using acousto-optical modulators (AOMs), driven by RF frequency generators. Piezo mirror mounts on the modulation bench are used for an offset phase lock between the interferometer beams. The phase readout system is a modified LISA Pathfinder style phasemeter, which can perform phase measurements at three heterodyne frequencies simultaneously and provides the control signals for the offset phase locks.

Opto-mechanical components used on the baseplate and in the TS design such as wave plate holders, photodiode mounts and beam dumps are all designed with thermal stability and thermal-mechanical stress in mind. The photodiode mounts used for the science interferometer and the on-board CQP, glued directly to the Zerodur® optical baseplate, use a combination of titanium and aluminium in their construction which will compensate for any thermal expansion and ensure that the centre position of the mounted photodiode remains stable at the µm-level. The photodiode packages were electrically and thermally isolated by mounting in MACOR ceramic.

The TS has a 280 mm x 280 mm Zerodur® baseplate of thickness 35 mm and mass 7 kg that is polished for bonding on both sides. It has a hole through which the periscope optics direct the beams to and from the OB.
Fig. 4 shows the schematic of the TS layout. Two additional beam splitters are used in the reference interferometer to create four read-out ports to maximize the system flexibility. These are equipped with a reference QPD (ref QPD), a reference single element photo diode (SEPD) labelled ref SEPD, a phase camera and an auxiliary photo diode (REF AUX). Each port is path-matched to the Rx clip.
Furthermore, the TS features two Rx-beam sources - one Gaussian (from a fibre injector optical subassembly (FIOS)) labelled RX Gauss FIOS and one flat-top - both of which can be steered via the on-bench actuators. The flat-top generator consists of a large fibre coupler producing a 9 mm-radius Gaussian beam that is clipped by an apodized aperture. The aperture is optimized to minimize diffraction and result in a flat phase and intensity over a diameter of three millimeter at the plane of the Rx beam clip on the OB. An LO beam from a FIOS provides the required ultra-stable reference for the TS. A polarizing beam splitter and half-wave-plate facilitate the required polarization multiplexing between the OB and TS.

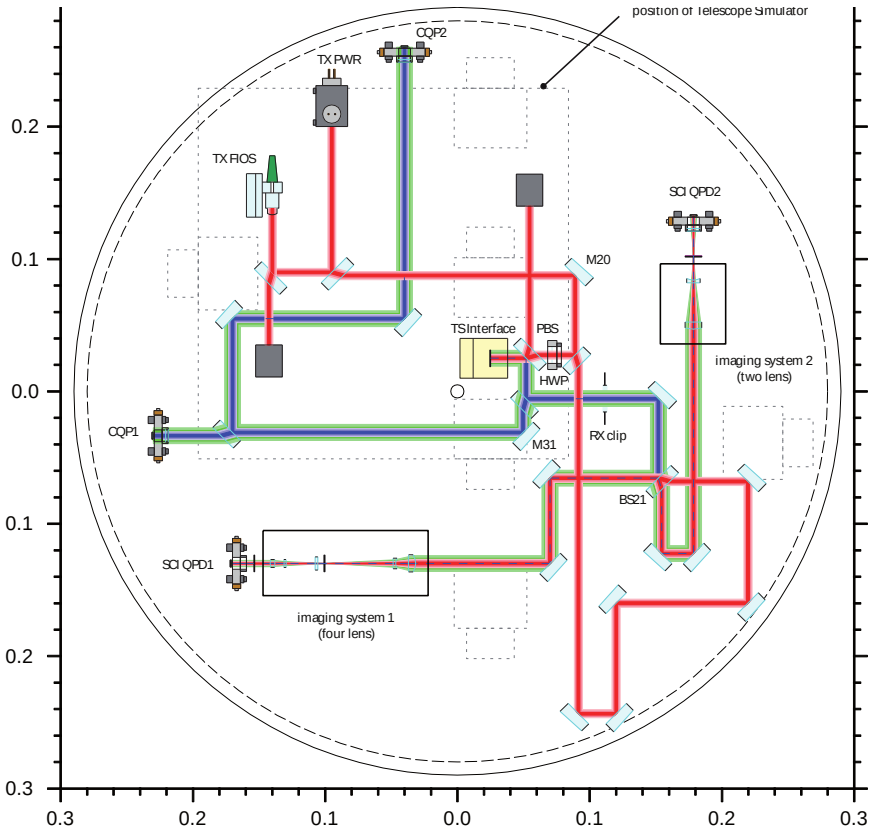

Fig. 3 Optical layout of the optical bench (OB) and labelling of the key components. The imaging systems in front of the SCI (science interferometer) quadrant photo diodes (QPDs) are on separate baseplates and can be exchanged. Here, one four-lens and one two-lens imaging system is shown. The Rx (green) and the LO (blue) beam are produced on the telescope simulator and interfered with the Tx (red) beam from the TX FIOS. The two CQP (calibrated quadrant photo diode pair) photo diodes are used for the alignment. The dashed outline is indicating the position of the telescope simulator in the nominal and the flipped position. The scale is in meters.

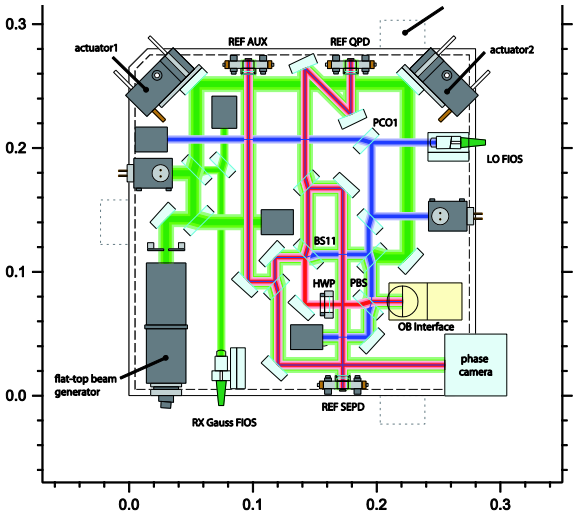

Fig. 4 Optical layout of the telescope simulator (TS) and labelling of key components. Either the Rx flat top from the flat-top generator or the Rx Gauss from the Rx FIOS can be used. The Rx beam (green) is tilted by two piezo driven actuators and combined with the stable reference LO beam (blue). The reference interferometer has four readout ports with three different photo diodes and a phase camera. The REF SEPD is a small pinhole photo diode, the REF QPD is a quadrant photo diode and the AUX SEPD is a big single element photo diode. The dashed outlines are the positions of the feet for the tip-tilt mount to align the telescope simulator. The scale is in meters.

Fig. 5 shows a photograph of the eLISA OB test bed. The TS is placed on top of the OB.

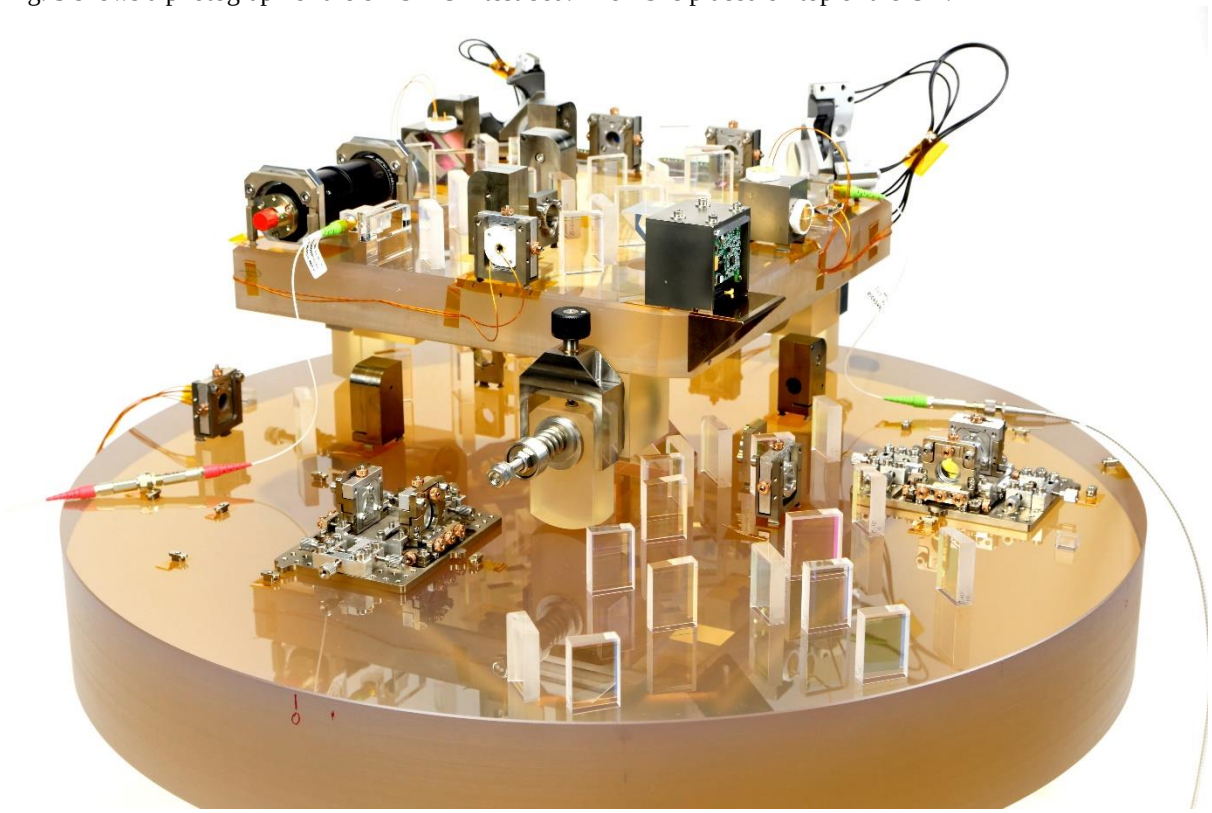

Fig. 5 Photograph of the eLISA Optical Bench test bed.
The telescope simulator is placed on top of the optical bench.

D. Imaging system design

Two different types of imaging systems were designed against requirements representative for eLISA. A magnification factor of 0.4 was chosen to detect most power of 2 mm diameter beams on the OB on 1 mm diameter photo diodes. A four-lens imaging system was designed and built using a classical optics approach (pupil plane imaging system). However, in this report we restrict ourselves to the other type of imaging system: the two-lens imaging system. Its central idea is to allow a divergent exit beam for a collimated input beam and require only vanishing beam walk, vanishing tilt-to-length coupling, and a suitable beam size on the QPD. This allows a reduction in the number of lenses required while preserving the magnification factor of the beam size. The two-lens imaging systems were designed by using the framework IfoCad [13]. A list of off-the-shelf spherical fused silica lenses was used as starting point. For each combination of two lenses, the distance between both lenses as well as the distance between the second lens and QPD was varied until a measurement beam tilted by 100 µrad hit the centre of the QPD at an angle of 250 µrad (0.4 magnification). For any solution found, the path length signal and its slope (tilt-to-length coupling) were computed. The solution with the best performance was chosen. The resulting set of lenses and parameters is shown in Tab. 1.

E. Telescope simulator alignment

Before imaging systems on the OB were investigated, the TS was carefully aligned in five degrees of freedom (DoF): in three translational and two rotational DoF (tip and tilt, for the yaw axis a coarse alignment was sufficient). The alignment was performed by only operating the LO beam on the TS. It was detected by the QPD pair (CQP) on the OB and centred on both QPDs (to single µm) by changing the TS position.
Then, the lateral position of the reference photo diode on the TS was aligned. The reference photo diode is a small pinhole single-element photo diode. For this purpose a temporary QPD was placed in the Rx clip on the OB and centred on the LO beam. The temporary QPD was then replaced by a single-element photo diode (identical to the reference photo diode) aligned to the centre of the QPD to a few µm. This temporary pinhole was now centred on the LO beam. The actuators on the TS were commanded to rotate the Rx beam around the temporary pinhole photo diode. This photo diode and the reference pinhole photo diode were read out and their difference phase signal was analysed. If the reference photo diode was laterally shifted with respect to the temporary pinhole, then a linear coupling in the difference phase between both diodes over beam angle was visible. This linear coupling

Tab. 1 Specifications of the two lens imaging system

		Lens 1	Lens 2	QPD
Name		PLCX-12.7-20.6-UV-1064	PLCC-10.0-12.9-UV-1064	
Position	mm	350.051	385.109	434.673
Primary curvature	1/mm	0.0485601	0.0	
Secondary curvature	1/mm	0.0	−0.0774931	
Center thickness	mm	5.3	2.0	
Substrate radius	mm	6.35	5.0	
Refractive index	1	1.44963	1.44963	
QPD aperture diameter	mm			0.9
Slit diameter	µm			20
Min. ghost power suppr.	1			$1.36 \cdot 10^{-7}$

was then reduced by laterally shifting the reference photo diode. As a result of the alignment procedure the reference pinhole photo diode was laterally aligned to the temporary pinhole within a few µm.

II. RESULTS

Initial measurements were made without any imaging systems. Fig. 6 shows the effect of beam angle changes on path length changes between science interferometer QPDs and reference PD and their slopes. For each QPD the phase signals of their four segments were averaged (see Eq. (5) in [14]). From this average the phase signal of the reference single element photo detector was subtracted. The phase difference $\Delta\varphi$ was converted to an optical length change Δs according to $\Delta s = \lambda/2\pi \cdot \Delta\varphi$ where λ=1064 nm is the laser wavelength.
Three laser beams (Rx,LO,Tx) were incident on the photo detectors and led to three heterodyne signals (A: Rx-Tx, B: LO-Tx, C: Rx-LO). Both LO and Tx beams were static, while the Gaussian Rx beam was tilted around the Rx clip. Starting from angle zero the Rx beam was tilted towards negative angles, rotated back to angle zero, continued to positive angles and returned to angle zero again. Both length changes in signals A and C show a parabolic shape as is expected [15]. Signal B, expected to remain constant, shows a temperature-driven drift of the TS height that was mitigated during measurements involving the imaging systems under test.
The graphs on the right were calculated numerically from the path length changes. For each data point, five path length data points were used in the slope calculation. The tilt-to-length coupling must not exceed ±25 µm/rad for beam angles in the range ±300 µrad. Without imaging systems this requirement is violated up to a factor of six.

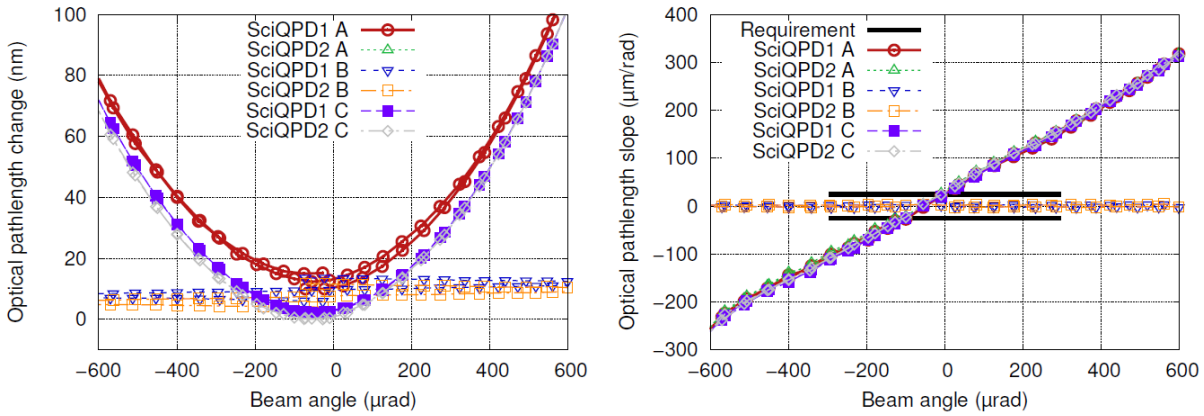

Fig. 6 Performance measurement of the entire test bed without imaging system. On the left the path length change as a function of the tilt angle is shown for the three heterodyne signals (A: Rx-Tx, B: LO-Tx, C: Rx-LO) on both science interferometer diodes respectively. Signal B is the superposition between the two static beams and therefore shows no reaction to the beam tilt. Signal A and C are the superposition between the tilting beam and one of the static beams. Both signals show the expected quadratic tilt-to-length (TTL) coupling, due to the longitudinal mismatch between point of rotation and the science interferometer detectors. The signals from the different photo detectors show very similar signals, as intended. In the right plot, the slope of the path length signal is plotted over the beam angle to relate the measurement with the requirement of 25µm/rad, which is clearly not achieved in this scenario without imaging system.

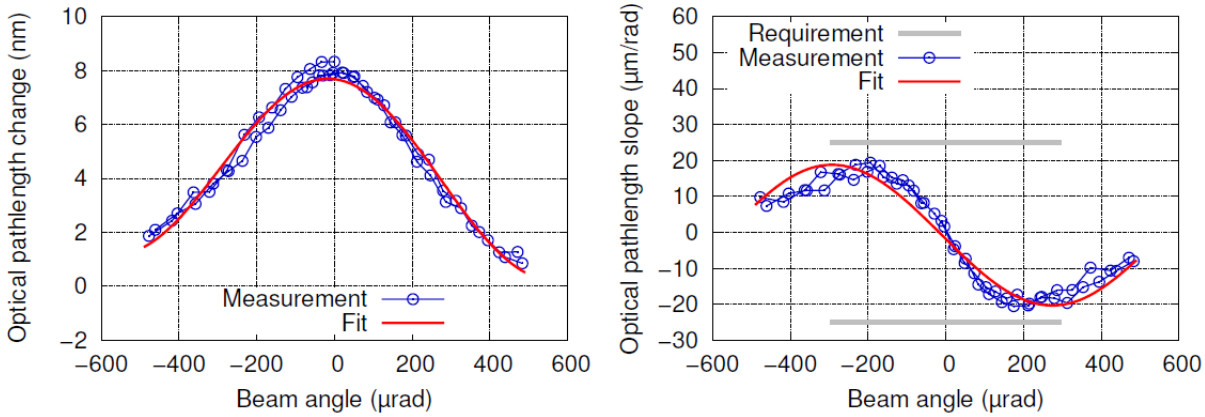

Fig. 7 Two-lens imaging system: nominal performance with Gaussian RX beam and 1m focal length lens in front of RX FIOS on telescope simulator. Left: Path length change vs. beam angle, right: Slope of path length change vs. beam angle.

Fig. 7 shows the nominal performance of the two-lens imaging system placed in front of SciQPD1 when the Gaussian RX beam was used with an additional 1m focal length lens in front of the RX FIOS. The left side shows the path length change between the averaged sum phase SciQPD1 signal and the reference SEPD signal versus beam angle between Rx and Tx beam. The right side shows the slope of the path length change versus beam angle. For beam angles in the range ±300 µrad the measured coupling is well within the requirement of ±25 µm/rad.

III. CONCLUSIONS

Tilt-to-length (TTL) coupling has a large contribution to the evolved Laser Interferometer Space Antenna (eLISA) noise budget and is planned to be suppressed by imaging systems placed on the OB in front of the interferometer readout photo diodes.
We have designed and built an imaging system to suppress this coupling. We have designed and constructed an optical test bed to experimentally investigate tilt-to-length coupling. The test bed consists of an optical bench (OB) and a telescope simulator (TS). The OB encompasses the measurement interferometer, the TS the reference interferometer. We avoid TTL coupling in the reference interferometer by using a small photo diode placed in a copy of the beam rotation point. On the TS we generated a Gaussian beam that mimicked the beam to read out distance changes between OB and test mass. An initial measurement of tilt-to-length coupling without imaging systems shows that the test bed is operational. The measured coupling exceeds the requirement of ±25 µm/rad for beam angles within ±300 µrad by a factor of up to six. This demonstrates that reduction of tilt-to-length (TTL) coupling is required. When using a two-lens imaging system, the requirement is met.

IV. ACKNOWLEDGEMENTS

We acknowledge funding by the European Space Agency within the project “Optical Bench Development for LISA” (22331/09/NL/HB), support from UK Space Agency, University of Glasgow, Scottish Universities Physics Alliance (SUPA), and support by Deutsches Zentrum für Luft und Raumfahrt (DLR) with funding from the Bundesministerium für Wirtschaft und Technologie (DLR project reference 50 OQ 0601). We thank the German Research Foundation for funding the cluster of Excellence QUEST - Centre for Quantum Engineering and Space-Time Research.

REFERENCES

[1] The eLISA Consortium: P. A. Seoane et al., “The Gravitational Universe,”arXiv e-prints 1305.5720, 2013
[2] NGO Assessment Study Report, ESA document ESA/SRE (2011) 19,
URL http://sci.esa.int/jump.cfm?oid=49839, 2011
[3] LISA Project, “Laser Interferometer Space Antenna (LISA) Measurement Requirements Flowdown Guide,” internal report number LISA-MSE-TN-0001, URL http://lisa.nasa.gov/Documentation/LISA-MSE-TN-0001 v2.0.pdf, 2009
[4] S. Schuster et al. „Experimental demonstration of reduced tilt-to-length coupling by a two-lens imaging system,” Opt. Express 24(10):10466–10475, 2016.
URL http://www.opticsexpress.org/abstract.cfm?URI=oe-24-10-10466

[5] M. Chwalla et al. “Design and construction of an optical test bed for eLISA imaging systems and tilt-to-length coupling,” arXiv e-prints 1607.00408, 2016
[6] G. Heinzel et al., “The LTP interferometer and phasemeter,” Class. Quantum Grav. 21 S581-S587, 2004
[7] O. Gerberding et al., “Readout for intersatellite laser interferometry: Measuring low frequency phase fluctuations of high-frequency signals with microradian precision,” Review of Scientifc Instruments, 86, 074501, 2015
[8] M. Armano et al., “Sub-Femto-*g* Free Fall for Space-Based Gravitational Wave Observatories: LISA Pathfinder Results” Phys. Rev. Lett., 116:231101, 2016
[9] L. d'Arcio et al., “Optical bench development for LISA,” Proc. of the International Conf. on Space Optics, 2010
[10] M. Tröbs et al., “Testing the LISA optical bench,” Proc. of the International Conference on Space Optics, 2012
[11] E. D. Fitzsimons et al., “Precision absolute positional measurement of laser beams,” Appl. Opt. 52 2527-2530, 2013
[12] A. M. A. van Veggel, C. J. Killow, “Hydroxide catalysis bonding for astronomical instruments,” Advanced Optical Technologies 3 293-307, 2014
[13] G. Wanner et al., “Methods for simulating the readout of lengths and angles in laser interferometers with Gaussian beams,“ Optics Communications 285 4831 – 4839, 2012
[14] G. Wanner et al. “A brief comparison of optical pathlength difference and various definitions for the interferometric phase,” Journal of Physics: Conference Series 610, 012043, 2015
[15] S. Schuster et al. “Vanishing tilt-to-length coupling for a singular case in two-beam laser interferometers with Gaussian beams,” Appl. Opt. 54 1010-1014, 2015